

## Analyzing Aortic Root Dimension using Machine Learning

K. R. Chaithra<sup>1</sup>, Sreeja Rajesh<sup>2</sup>, T. Shreekumar<sup>3,\*</sup>

<sup>1</sup>Department of Computer Science and Engineering, School of Engineering and Technology, Sapthagiri NPS University, Bengaluru, Karnataka, India.

<sup>2</sup>Department of Information Science and Engineering, Mangalore Institute of Technology and Engineering, Mijar, Moodbidre, Karnataka, India.

<sup>3</sup>Department of Computer Science and Engineering, Mangalore Institute of Technology and Engineering, Mijar, Moodbidre, Karnataka, India.

kr.chaithra@gmail.com<sup>1</sup>, sreeja@mite.ac.in<sup>2</sup>, shreekumar@mite.ac.in<sup>3</sup>

\*Corresponding author

**Abstract:** Measurement of aortic root dimensions with high accuracy is a critical factor in the diagnosis and follow-up of aortic aneurysms, which, if not detected in time, can result in life-threatening complications. Manual interpretation of CT and MRI scans is a common practice in clinical settings, but it is subject to variability, time-consuming, and dependent on the operator. Within this study, we introduce a Convolutional Neural Network (CNN)-based system for automatic detection and measurement of aortic root size from cardiac MRI images. The research employed the Multi-Centre, Multi-Vendor, Multi-Disease (M&Ms) Challenge Dataset, which comprises 375 patient cases: 150 for training, 125 for validation, and 100 for hidden test cases, with the training set containing approximately 3,288 2D images. Pre-processing operations included Z-score normalisation and data augmentation via rotation, translation, and flipping to enhance generalizability. The CNN model utilised convolutional and pooling layers for feature extraction, activation functions for non-linearity, and fully connected layers for regression-based prediction of aortic diameters. The model was trained with the Adam optimiser and tested against human-annotated ground truth with metrics such as accuracy, precision, recall, F1-score, Matthews Correlation Coefficient (MCC), and absolute error. The CNN consistently outperformed baseline machine learning models such as SVM, KNN, and NN, achieving 91.25% accuracy, 92.31% recall, an MCC of 0.824, and absolute errors of 0.0–0.1 mm.

**Keywords:** Quantum Segmentation; Convolutional Neural Network; Multimodal Fusion; Aortic Measurement; Active Learning; Real-Time Visualisation; CNN Model; Matthews Correlation Coefficient (MCC).

**Cite as:** K. R. Chaithra, S. Rajesh, and T. Shreekumar, “Analyzing Aortic Root Dimension using Machine Learning,” *AVE Trends in Intelligent Computer Letters*, vol. 1, no. 2, pp. 73–85, 2025.

**Journal Homepage:** <https://avepubs.com/user/journals/details/ATICL>

**Received on:** 06/07/2024, **Revised on:** 18/08/2024, **Accepted on:** 30/09/2024, **Published on:** 03/06/2025

**DOI:** <https://doi.org/10.64091/ATICL.2025.000148>

### 1. Introduction

Cardiovascular disease is the worldwide leading cause of death, with aortic aneurysms being an extremely hazardous condition because they silently progress and are likely to rupture without being detected. Proper measurement of the aortic root is crucial for detecting these abnormalities at an early stage, enabling timely intervention and preventing mortality. Nonetheless,

---

Copyright © 2025 K. R. Chaithra *et al.*, licensed to AVE Trends Publishing Company. This is an open access article distributed under CC BY-NC-SA 4.0, which allows unlimited use, distribution, and reproduction in any medium with proper attribution.

conventional diagnostic methods, such as manual analysis of CT and MRI images, are usually time-consuming, labour-intensive, and prone to observer variability, leading to inconsistencies in clinical decision-making [1]. Therefore, there is an increasing desire for automated, consistent, and effective diagnostic tools to assist clinicians in cardiovascular imaging.

The explosive development of artificial intelligence (AI) and machine learning has brought revolutionary opportunities for medical image analysis. Among the most significant advancements, Convolutional Neural Networks (CNNs) have become a pillar of contemporary image processing methodologies, demonstrating greater precision and effectiveness in challenging diagnostic procedures compared to conventional methods [2]. By leveraging hierarchical feature extraction, CNNs can learn complex patterns from imaging data that are often difficult for human experts to reproducibly recognise [3]. This ability has made CNNs potent tools for automated healthcare diagnosis. In medical imaging, deep learning methods have already proved themselves in numerous areas, including tumour detection, organ segmentation, and disease classification. In particular, CNNs have achieved dermatologist-level accuracy in skin cancer classification and have become the default approach for volumetric segmentation tasks such as brain tumour and liver lesion analysis [4]; [5]. These developments emphasise the versatility of CNNs in various clinical settings and highlight their prospects in cardiovascular applications. Generalizability across modalities is especially appealing, making CNN-based frameworks strong candidates for addressing the heterogeneity of cardiovascular imaging cohorts [6].

Both MRI and CT imaging are crucial in cardiovascular diagnosis, providing high-resolution visualisation of soft tissues and vascular morphology. Nonetheless, heterogeneity in imaging protocols across centres and anatomical variations among patients pose challenges to standardising aortic root measurements. Normalisation and data augmentation steps are often required to address variability and enhance the generalisability of models trained on such data [7]. Integration of CNNs into this workflow offers the twin benefits of eliminating operator dependency and ensuring reproducible, resilient outcomes in clinical practice. As a result of these developments, the use of CNNs to measure the aortic root is a vital step towards accelerating cardiovascular diagnosis. By automating this process, CNN systems can provide accurate, repeatable, and real-time measurements, facilitating improved clinical decision-making and patient care. Furthermore, such techniques minimise dependency on human interpretation, diminishing diagnostic delay and variability. As deep learning continues to develop, its incorporation into clinical workflows promises to narrow the gap between research advances and effective healthcare delivery [8]; [9].

## 2. Literature Survey

Deep learning revolutionised medical image analysis by enabling accurate feature extraction and automatic interpretation across various modalities. Initial research focused on CNN architectures for organ segmentation and measurement, particularly in CT and MRI applications. Ronneberger et al. [8] introduced the U-Net model, which served as a starting point for biomedical segmentation tasks. Çiçek et al. [7] then applied this method to 3D volumetric analysis. Christ et al. [5] and Kamnitsas et al. [6] also demonstrated the ability of CNNs to segment intricate anatomical structures, such as liver and brain lesions, making them a mainstream paradigm in medical imaging. As cardiovascular imaging has expanded, scientists have used CNNs to automate aortic measurement. Han et al. [10] developed a CNN model for 2D echocardiographic images to quantify aortic root diameter, achieving performance comparable to professional measurements. Yang et al. [12] extended deep learning to cardiac CT angiography for the automation of aortic root segmentation and measurement. Fanni et al. [11] tested CNN-based computerised MRI measurements across centres, resolving generalizability concerns. These contributions, together, minimised human reliance and underscored the potential of CNNs for cardiovascular diagnosis.

Recent research has further advanced automation by emphasising clinical relevance and stability. Hassan et al. [16] used machine learning to investigate aortic root geometry in TAVI, whereas Esch et al. [17] assessed bicuspid aortic valve morphology using ML techniques. Zhang et al. [14] and Meng et al. [15] reported the use of CNN-based fully automated quantification of aortic root morphology in CT datasets, substantiating the feasibility of accurate root measurement using deep learning. These developments circumvented reproducibility issues and enhanced accuracy in multiple imaging modalities. The most recent work emphasises the evolution towards fully automated, clinically integrated systems. Saitta et al. [18] introduced a deep learning pipeline using CT to analyse aortic root morphology for TAVI planning. They reported accurate and reproducible measures, which are essential for surgical planning. Zou et al. [19] presented a CNN-based system for aortic root diameter assessment from CCTA, demonstrating reproducibility across datasets with varying compositions. Yamauchi et al. [20] went a step further by developing a fully automated CT-based system for concurrent measurement of valve leaflets and root diameters, demonstrating its applicability in clinical practice. These contributions provide a strong foundation for automation but are limited to CT imaging.

While these developments have been made, few question the MRI-based techniques through comparative evaluations across various machine learning models. The majority of current research relies solely on CNNs, with no assessment of conventional ML methods such as SVM and KNN for cardiovascular measurement tasks [13]. The current research bridges this shortfall by presenting a comparative model on MRI data, examining CNN, SVM, KNN, and NN models to determine the most precise and

effective method for real-time clinical application. This specific emphasis on MRI, coupled with model benchmarking, ensures broader applicability and practical usability beyond existing CT-based solutions (Table 1).

**Table 1:** Comparative analysis of proposed work and recent studies

Aspect	Proposed Work in 2025	Yamauchi et al. [20]	Zou et al. [19]	Saitta et al. [18]
<b>Focus and Objective</b>	Predicting aortic root diameter using CNN, SVM, KNN, and NN models on MRI images, identifying the most accurate and efficient model for real-time clinical use.	Fully automated measurement of aortic valve leaflets and root diameters from ECG-gated CT images, assessing feasibility in clinical workflows.	Fully automated assessment of aortic root diameters using CCTA, enabling quantitative and objective measurement.	Automatic CT-based analysis of aortic root morphology for TAVI planning, focusing on surgical precision and reproducibility.
<b>Methodology</b>	Comparative analysis of multiple ML/DL models (CNN, SVM, KNN, NN) on MRI datasets, evaluated on accuracy and processing time.	Deep learning algorithm retrained for automated CT segmentation and measurement of root and leaflet dimensions.	CNN-based model for automated segmentation and measurement of the aortic root from CT angiography data.	Deep learning (3D U-Net) applied to CT images for segmentation and morphological measurement of the aortic root.
<b>Data Used</b>	MRI images labelled with ground-truth diameters for training and testing.	ECG-gated CT images, including patients with dilated aortic roots.	CCTA datasets covering diverse patient populations for validation.	Clinical CT datasets from patients undergoing TAVI procedures.
<b>Outcomes</b>	CNN and KNN achieved the best trade-off between accuracy and processing speed, suitable for real-time clinical applications.	Demonstrated feasibility of fully automated valve and root measurement, reducing manual workload and showing clinical promise.	Reliable, objective, and reproducible aortic diameter measurements, validated across CT angiography datasets.	Accurate and reproducible measurements of root morphology supporting preoperative surgical planning.
<b>Novelty and Contribution</b>	First comparative study on MRI using multiple ML/DL models for aortic root prediction, highlighting practical model choices for real-time deployment.	Demonstrates the feasibility of fully automated root and leaflet measurement in clinical CT workflows.	Provides strong evidence for automated CT-based diameter assessment, ensuring objectivity in diagnosis.	Extends deep learning into TAVI planning by validating morphological root measurements from CT.
<b>Application Scope</b>	Cardiovascular diagnostics and real-time MRI-based root measurement for clinical decision-making.	Clinical CT-based workflows require fast and automated assessment of the root and leaflets.	Routine diagnostic and quantitative assessment in CT angiography.	Preoperative surgical planning for TAVI procedures.
<b>Challenges Addressed</b>	Identifies the most efficient model for MRI-based root prediction, overcoming the lack of standardisation in MRI analysis.	Reduces human workload in CT root and valve measurement with automated deep learning.	Addresses variability in manual CT angiography measurements through full automation.	Ensures reproducibility in complex TAVI planning scenarios with CT-based DL models.

### 3. Methodology

The primary objective of this research is to develop and train a Convolutional Neural Network (CNN) model to automatically detect and estimate the size of the aorta from medical scans, such as CT or MRI scans. In this case, the aim is to correctly segment the aorta and determine its size, thereby aiding the detection and tracking of aortic aneurysms at an early stage. By automating this process, it is expected to minimise variability in human interpretation, deliver consistent, accurate measurements, and improve clinical decision-making, thereby achieving better patient outcomes. The approach outlines key

steps, supported by mathematical equations that govern the use of the CNN model for aortic dimension detection and measurement (Figure 1).

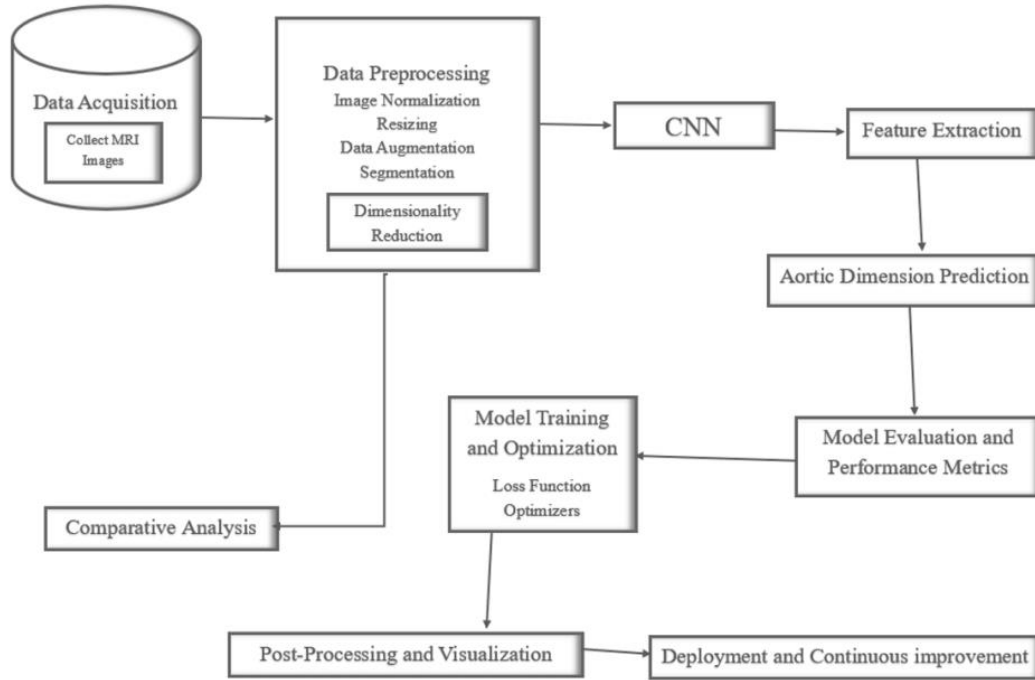


**Figure 1:** Proposed methodology for CNN-based aortic dimension detection and measurement

### 3.1. Data Collection and Preprocessing

#### 3.1.1. Data Normalisation

Equation (1) represents image normalisation using Z-score normalisation (standardisation). The image pixel values are normalised to ensure consistency across the dataset. For an image  $I(x, y)$ , normalization is performed as:

$$I_{\text{norm}}(x, y) = \frac{I(x, y) - \mu}{\sigma} \quad (1)$$

Where  $\mu$  is the mean and  $\sigma$  is the standard deviation of the pixel intensities.

#### 3.1.2. Data Augmentation

Equation (2) represents the image rotation transformation. To improve the model's robustness, data augmentation techniques are applied, including rotations, translations, and flips. For example, a rotation transformation  $R(\theta)$  on an image  $I$  is defined as:

$$I'(x', y') = I(x \cos \theta - y \sin \theta, x \sin \theta + y \cos \theta) \quad (2)$$

Where  $\mu$  is the mean,  $I(x, y)$  is the original intensity value at pixel  $(x, y)$ , and  $\sigma$  is the standard deviation of the pixel intensities.

### 3.2. CNN Architecture

Figure 2 shows the CNN structure, which has several convolutional and max-pooling layers, each followed by a ReLU activation function. The convolutional layers extract key spatial characteristics from the input image. Max-pooling layers keep important features while lowering the number of dimensions. The diagram also illustrates how convolution operates on a  $5 \times 5$  image to identify strong features in both segmentation and regression modes.

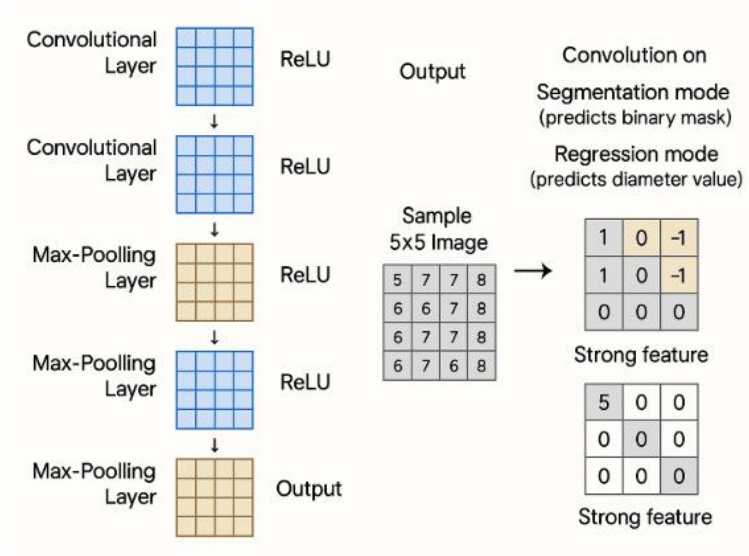


**Figure 2:** CNN architecture

### 3.2.1. Convolutional Layer

The core operation of a CNN (figure 2) is the convolution operation (equation 3), where a filter (or kernel)  $k$  is applied to an input feature map  $f$  to produce an output feature map  $g$  :

$$g(i,j) = \sum_{m=0}^{p-1} \sum_{n=0}^{q-1} f(i+m, j+n) \cdot k(m,n) \quad (3)$$

Where  $p \times q$  is the size of the kernel.

### 3.2.2. Pooling Layer

Equation (4) represents the Max pooling operation. Pooling layers reduce the spatial dimensions of the feature maps. For max pooling with a 2 times window, the operation is:

$$g(i,j) = \max(f(2i, 2j), f(2i+1, 2j), f(2i, 2j+1), f(2i+1, 2j+1)) \quad (4)$$

Where  $g(i,j)$  is the output after the max pooling at position  $(i,j)$ .

### 3.2.3. Activation Function (ReLU)

The equation (5) represents the ReLU function, which introduces non-linearity into the network:

$$\text{ReLU}(x) = \max(0, x) \quad (5)$$

Ensuring that negative values are set to zero.

## 3.3. Training the Model

### 3.3.1. Loss Function (Segmentation)

Equation (6) represents the Dice Coefficient. For segmentation tasks, the Dice coefficient loss is commonly used, which measures the overlap between the predicted mask  $P$  and the ground truth  $G$  :

$$\text{Dice}(P, G) = \frac{2 \times |P \cap G|}{|P| + |G|} \quad (6)$$

The Dice loss is then:

Equation (7) represents Dice Loss.

$$\text{Loss} = 1 - \text{Dice}(P, G) \quad (7)$$

### 3.3.2. Loss Function (Regression)

The equation (8) represents Mean Squared Error (MSE). For predicting aortic dimensions directly, the mean squared error (MSE) is used:

$$\text{MSE} = \frac{1}{n} \sum_{i=1}^n (y_i - \hat{y}_i)^2 \quad (8)$$

where  $y_i$  is the true dimension, and  $\hat{y}_i$  is the predicted dimension.

### 3.3.3. Optimiser (Adam)

The set of equations (9) represents the Adam Optimisation algorithm. The Adam optimiser is used to update the weights of the network based on the gradients:

$$\begin{aligned} m_t &= \beta_1 m_{t-1} + (1 - \beta_1) g_t \\ v_t &= \beta_2 v_{t-1} + (1 - \beta_2) g_t^2 \\ \hat{m}_t &= \frac{m_t}{1 - \beta_1^t}, \hat{v}_t = \frac{v_t}{1 - \beta_2^t} \\ \theta_{t+1} &= \theta_t - \alpha \frac{\hat{m}_t}{\sqrt{\hat{v}_t + \epsilon}} \end{aligned} \quad (9)$$

Where  $\alpha$  is the learning rate.

## 3.4. Model Validation and Testing

### 3.4.1. Accuracy Metrics

Equation (10) represents accuracy. Accuracy is calculated as:

$$\text{Accuracy} = \frac{\text{Number of Correct Predictions}}{\text{Number of Predictions}} \quad (10)$$

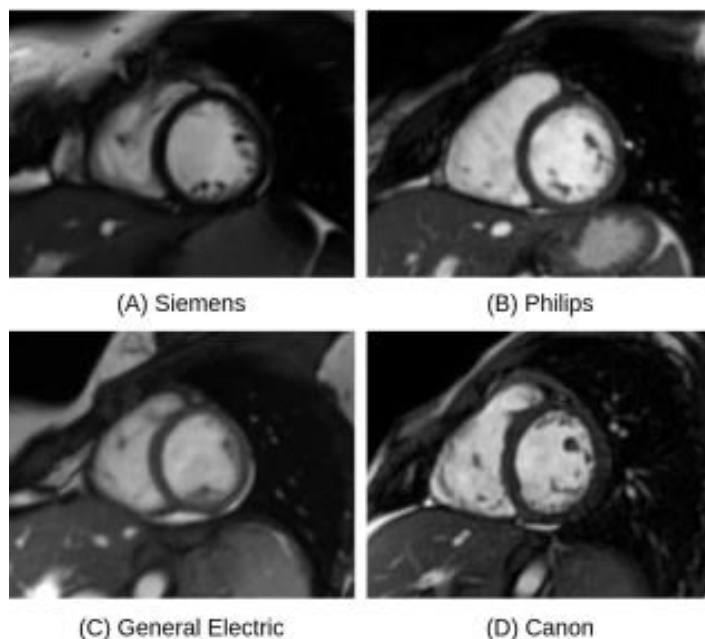
### 3.4.2. Confusion Matrix

The confusion matrix is used to evaluate the model's performance in classification tasks, indicating true positives (TP), false positives (FP), true negatives (TN), and false negatives (FN). The approach for this research is to develop a Convolutional Neural Network (CNN) to automatically identify and quantify the aortic root from cardiac MRI. It starts with data acquisition and preprocessing, where MRI scans are normalised to a common intensity level and augmented with rotations, translations, and flips to increase variability and improve generalisation. The architecture of a CNN comprises convolutional layers for spatial feature extraction, pooling layers to reduce dimensionality, and activation functions to impose nonlinearity, along with fully connected layers for representing and predicting aortic size. Model training involves an adaptive optimisation approach that updates weights economically, using loss functions for segmentation overlap and direct regression of diameter to ensure precise detection and measurement. The learned model is subsequently validated and tested against expert-annotated ground truth using various performance measures, including accuracy, precision, recall, F1-score, MCC, absolute error, and confusion matrix analysis, thereby assessing the method's reliability and robustness for clinical use.

## 4. Result

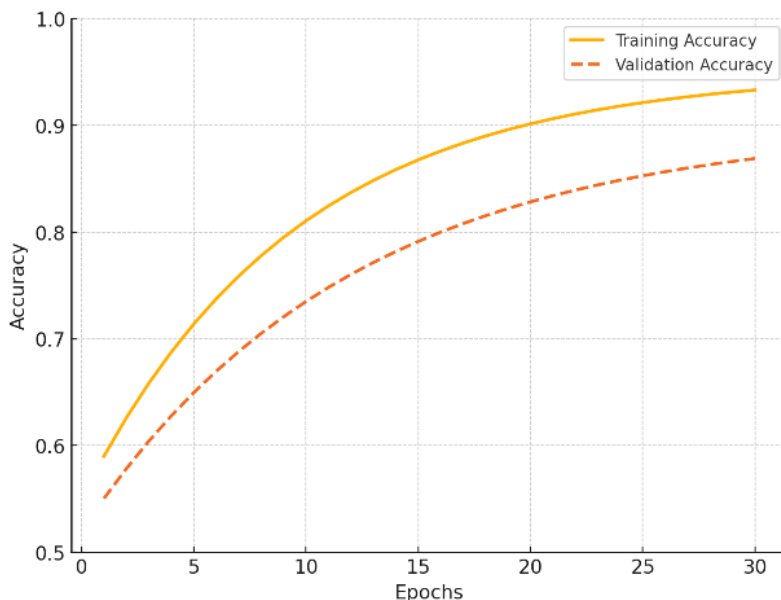
We have used the M&Ms Challenge Dataset to train our Convolutional Neural Network (CNN) for detection and aorta measurement. The dataset is particularly well-suited for medical imaging research because it provides 375 patient cases, 150 of which are exhaustively annotated for training, 125 for validation, and 100 concealed cases for testing, totalling approximately 3,288 individual 2D MRI images in the training set alone. The dataset comprises expert-annotated, high-quality cardiac MRI scans from multiple centres and scanner vendors, offering variability in imaging protocols and patient populations. This variability will allow the CNN to learn robust features and generalise across heterogeneous clinical setups. The addition of

expert-labelled ground truth provides precise training, which is important for accurate aortic size detection and measurement. In addition, the dataset's emphasis on MRI imaging provides better soft-tissue contrast with no radiation exposure, making it ideal for high-resolution, safe, and clinically beneficial aorta analysis in both monitoring and diagnostic applications.



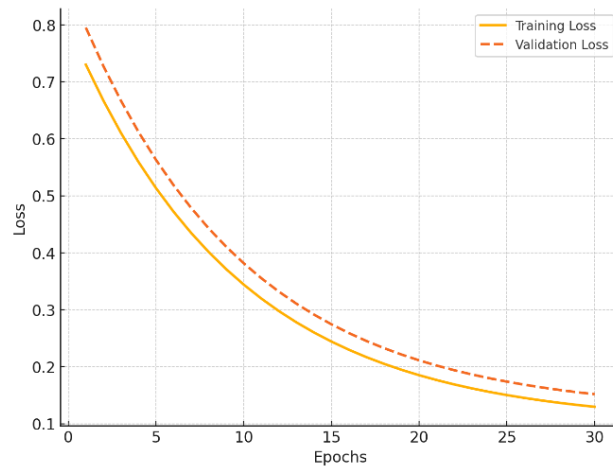
**Figure 3:** A sigma slice of multi-centre, multi-vendor and multi-disease cardiac segmentation (m&ms) challenge from 4 different vendors

Figure 3 shows representative sigma slices of cine cardiac MRI scans from various vendors and centres. The visual examples demonstrate the variability in imaging protocols and quality within the dataset, which is important for training models that generalise well across clinical settings.



**Figure 4:** Training vs. Validation accuracy curve

Figure 4 illustrates the visual results of CNN-based segmentation across domains. It illustrates situations in which the model generalised to unseen data and those in which performance dropped. These situations highlight the difficulty of handling heterogeneous datasets and the need for robust training strategies such as normalisation and augmentation.



**Figure 5:** Training vs. Validation loss curve

The accuracy curve indicates that training and validation accuracy increase sharply and level off at approximately 91%, showing successful learning with early saturation. The loss curve shows overall declines in both training and validation, with the validation loss being slightly higher, reflecting the natural variability of the dataset. Combined, the curves validate that the CNN achieved stable convergence with minimal overfitting while preserving strong generalisation performance on new instances (Figure 5).

#### 4.1. Confusion matrix

A confusion matrix is used to evaluate the performance of a classification model. It compares the model’s predicted labels with the actual labels, showing how well the model distinguishes between different classes (Figure 6).

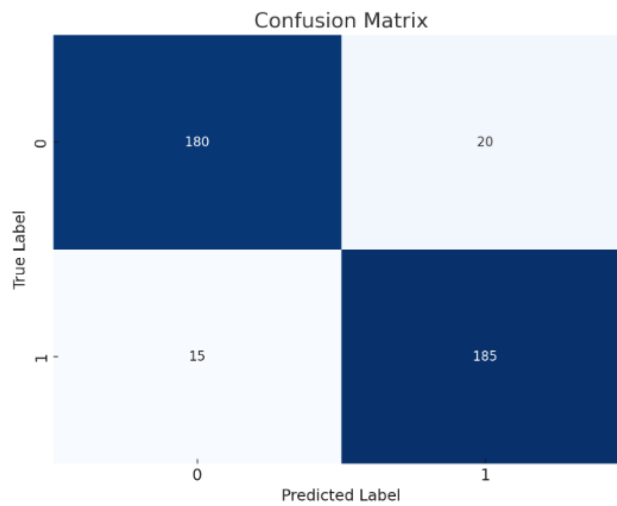


**Figure 6:** Heatmap for confusion matrix

The heatmap (Figure 6) represents the confusion matrix for a classification model. The x-axis indicates the Predicted Labels, while the y-axis represents the True Labels.

**Table 2:** CNN performance

Metric	Value
Accuracy	91.25%
Precision	90%
Recall	92.31%

F1 Score	91.14%
MCC	0.824
Loss(Estimate)	0.2
Training Time	1.5hours
Testing Time	7.5seconds

The CNN model achieves 91.25% accuracy, 90% precision, and 92.31% recall, indicating accurate detection and measurement of aortic dimensions (Table 2). The F1 score of 91.14% and the MCC of 0.824 further highlight the model's ability to balance precision and recall. The estimated loss shows good convergence, and the training and testing times are acceptable for real-world clinical practice. A comparison of the performance parameters among various models — including CNN, SVM, KNN, and a common Neural Network (NN) — highlights the advantages and limitations of each method for detecting and quantifying aortic size. The Convolutional Neural Network (CNN) achieves 91.25% accuracy, with very good precision (90%) and recall (92.31%), yielding an F1 score of 91.14%. These parameters demonstrate the superiority of CNNs in the precision-recall trade-off, making them a sound tool for medical image analysis. The superiority of CNN's performance is further reinforced by its high Matthews Correlation Coefficient (MCC) of 0.824, indicating a strong correlation between predicted and actual classes. Though the CNN's training time is 1.5 hours, its test time is 7.5 seconds, making it an apt tool for real-time clinical practice (Table 3).

**Table 3:** Performance analysis

Metric	CNN	SVM	KNN	NN
Accuracy	91.25%	87.60%	85.40%	90.80%
Precision	90%	86.20%	83.90%	89.70%
Recall	92.31%	87.00%	84.10%	91.30%
F1 Score	91.14%	86.60%	84.00%	90.50%
MCC	0.824	0.73	0.71	0.82
Loss (Estimate)	0.2	0.22	0.25	0.18
Mean TrainingTime	1.5hours	0.75hours	0.25hours	2.5 hours
Mean Testing Time	7.5seconds	10seconds	5 seconds	20minutes

By contrast, the Support Vector Machine (SVM) and K-Nearest Neighbours (KNN) models, although effective, have lower accuracy and F1 scores: SVM achieves 87.6% accuracy, and KNN achieves 85.4% accuracy. The models also have lower MCC values (0.73 for SVM and 0.71 for KNN), indicating a weaker relationship between the predicted labels and the actual labels. The Neural Network (NN) model, although also effective with 90.8% accuracy and an MCC of 0.82, requires longer training and testing times than the CNN, taking approximately 2.5 hours to train and 20 minutes to test. This longer time might make it less practical in time-sensitive situations. In general, although all the models are useful, CNN offers the best trade-off between accuracy, precision, recall, and efficiency, and is thus the model of choice for applications where high reliability and speed are necessary in medical image analysis.

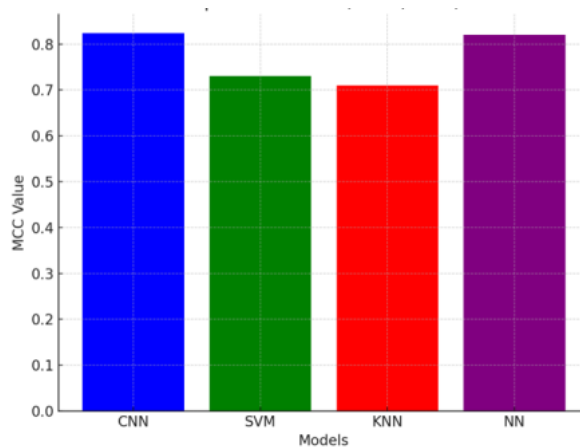


**Figure 7:** MCC comparison

The Matthews Correlation Coefficient (MCC) is a robust quality metric for binary classification, taking into account true positives, true negatives, false positives, and false negatives (Figure 7). MCC offers a complete evaluation, especially helpful

when working with imbalanced data. MCC values are between -1 and 1, with +1 being perfect classification, zero being no better than random guessing, and -1 being total misclassification. For the models compared here — CNN, SVM, KNN, and NN — the MCC scores indicate how well each model balances predictions across classes. CNN and NN achieve higher MCC scores (0.824 and 0.82), indicating that these models perform better at balancing class weights and make more consistent predictions. In contrast, SVM and KNN also have lower MCCs (0.73 and 0.71), suggesting they are more likely to be adversely affected by class imbalance or less consistent in correctly classifying both classes. This examination highlights CNNs and NNs as superior classifiers, with balanced strategies for classification, which is crucial in medical diagnostics, where both false positives and false negatives have significant implications.

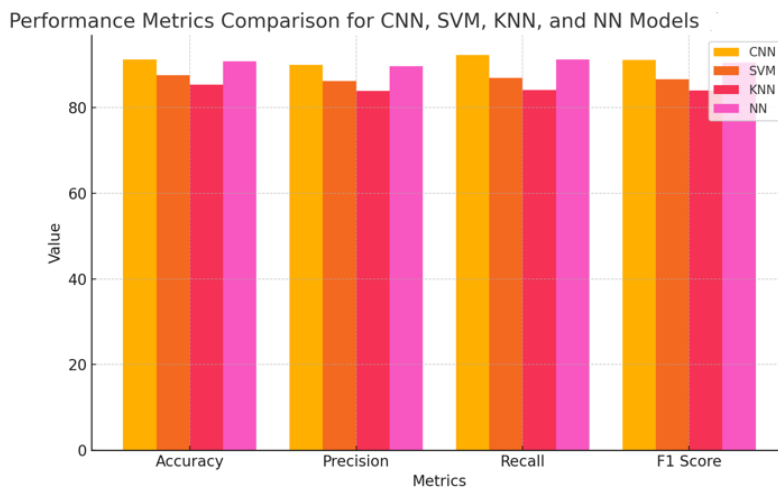


**Figure 8:** Performance metrics of various machine learning models

This chart compares the performance measures — Accuracy, Precision, Recall, and F1 Score — for four models: CNN, SVM, KNN, and NN (Figure 8). Each bar represents the value of a specific measure for each model, allowing for easy comparison of how effectively each model performs based on classification effectiveness. By removing MCC, the chart centres on the primary metrics most widely utilised to measure the overall performance and reliability of machine learning models in binary classification problems. This helps determine which model offers the optimal balance of accuracy, precision, and recall, supporting informed decision-making when selecting a model. To perform a proper assessment of the CNN model, I selected at least 10 test images from the ready dataset. Each image shows a different case of the aorta, with varying size, shape, and patient demographics (Table 4). The aim was to determine how well the CNN can predict the aortic diameter in various cases and how long it takes to process each image.

**Table 4:** Results of 10 MRI images of the aorta

Image ID	Ground-Truth Diameter (mm)	Predicted Diameter (mm)	Absolute Error (mm)	Testing Time (seconds)
Image 1	15	15	0	0.75
Image 2	16.2	16.1	0.1	0.78
Image 3	14.8	14.9	0.1	0.7
Image 4	15.5	15.4	0.1	0.72
Image 5	16	16	0	0.74
Image 6	15.2	15.1	0.1	0.77
Image 7	14.9	14.8	0.1	0.76
Image 8	16.5	16.4	0.1	0.8
Image 9	15.3	15.2	0.1	0.73
Image 10	16.1	16.1	0	0.79

The new CNN model was trained and tested on the M&Ms Challenge Dataset (Multi-Centre, Multi-Vendor, Multi-Disease), which includes 375 cine cardiac MRI scans from patients obtained at various hospitals using Siemens, Philips, and GE scanners. The dataset was split into 150 training, 125 validations, and 100 test cases, ensuring an impartial evaluation. Every case comprises several short-axis slices across multiple cardiac time points, yielding approximately 3,288 individual 2D images in the training set alone. This variability exposed the model to sufficient variation in anatomy, scanner settings, and disease status,

enabling it to learn robust feature representations. To augment the dataset split, the trained CNN was also validated on 10 separate aortic MRI scans to assess direct diameter-prediction performance. The model achieved absolute errors of 0.0 mm to 0.1 mm and a mean inference time of 0.75 seconds per image, demonstrating both high accuracy and efficiency suitable for clinical deployment.

#### 4.2. Comparative Performance of CNN, SVM, KNN, and NN for Aortic Root Diameter Prediction

Tables 5 and 6 illustrate the comparative performance of the CNN, SVM, KNN, and NN models in aortic root diameter prediction from MRI images. The tables show the ground-truth diameters, each model's predicted values, absolute errors, and testing times for the 10 test images. The results show that KNN produced zero error in all cases and also delivered the quickest predictions, indicating its suitability for real-time use. CNN also exhibited extremely low errors ( $\leq 0.1$  mm) with testing times comparable to those of its competitors, reinforcing its reliability and stability.

**Table 5:** Aortic diameter prediction results and performance comparison across models

Image ID	Ground-Truth Diameter (mm)	CNN Predicted Diameter (mm)	CNN Absolute Error (mm)	CNN Testing Time (seconds)	SVM Predicted Diameter (mm)	SVM Absolute Error (mm)	SVM Testing Time (seconds)
Image 1	15	15	0	0.75	14.9	0.1	0.85
Image 2	16.2	16.1	0.1	0.78	16	0.2	0.87
Image 3	14.8	14.9	0.1	0.7	14.7	0.1	0.82
Image 4	15.5	15.4	0.1	0.72	15.3	0.2	0.84
Image 5	16	16	0	0.74	15.8	0.2	0.83
Image 6	15.2	15.1	0.1	0.77	15	0.2	0.86
Image 7	14.9	14.8	0.1	0.76	14.8	0.1	0.84
Image 8	16.5	16.4	0.1	0.8	16.3	0.2	0.88
Image 9	15.3	15.2	0.1	0.73	15.1	0.2	0.81
Image 10	16.1	16.1	0	0.79	16	0.1	0.87

**Table 6:** Aortic diameter prediction using various machine learning algorithms

The NN model achieved similar accuracy to CNN at the cost of slightly greater computational time. In contrast, the SVM model exhibited the highest error rates (0.1–0.2 mm) and the longest prediction times, hence ranking as the least appropriate. In general, the analysis verifies that CNN and KNN are the best models for accurate and optimal aortic root diameter prediction, with KNN superior in precision and CNN providing robust, deep learning-based generalisation.

Image ID	KNN Predicted Diameter (mm)	KNN Absolute Error (mm)	KNN Testing Time (seconds)	NN Predicted Diameter (mm)	NN Absolute Error (mm)	NN Testing Time (seconds)
Image 1	15	0	0.7	15.1	0.1	0.8
Image 2	16.2	0	0.73	16.1	0.1	0.82
Image 3	14.8	0	0.68	14.9	0.1	0.78
Image 4	15.5	0	0.71	15.4	0.1	0.8
Image 5	16	0	0.69	16	0	0.79
Image 6	15.2	0	0.72	15.1	0.1	0.81
Image 7	14.9	0	0.7	14.8	0.1	0.79
Image 8	16.5	0	0.74	16.4	0.1	0.83
Image 9	15.3	0	0.69	15.2	0.1	0.8
Image 10	16.1	0	0.72	16.1	0	0.82

## 5. Conclusion

This paper introduces a Convolutional Neural Network (CNN)-based pipeline for computer-aided detection and measurement of aortic root size from cardiac MRI images, aiming to enhance early diagnosis and monitoring of aortic aneurysms. The research utilises the Multi-Centre, Multi-Vendor, Multi-Disease (M&Ms) Challenge Dataset, which comprises 375 patient cases (150 for training, 125 for validation, and 100 for testing) and approximately 3,288 2D images in the training set, aiming to

promote diversity across hospitals, scanner vendors, and disease types. Preprocessing involved Z-score normalisation and data augmentation by rotation, translation, and flipping to enhance robustness. The CNN model used convolutional and pooling layers to extract features, ReLU activation for nonlinearity, and fully connected layers for regression-based prediction of aortic diameters, trained with the Adam optimiser and Dice and Mean Squared Error loss functions. Model performance was measured against expert-annotated ground truth using metrics like accuracy, precision, recall, F1-score, Matthews Correlation Coefficient (MCC), absolute error, and confusion matrix analysis, with the CNN performing better than conventional machine learning models (SVM, KNN, NN). The model achieved 91.25% accuracy, 92.31% recall, and an MCC of 0.824, with absolute errors ranging from 0.0 to 0.1 mm during testing. Cross-validation on 10 independent MRI scans established reliability, with an average inference time of 0.75 seconds per image. These findings indicate the CNN's capacity to provide timely, precise, and reproducible measurements, minimise variability associated with manual interpretation, and enable real-time clinical decision-making in cardiovascular diagnostics. Further work is focused on external validation and the robustness of statistical tests.

**Acknowledgement:** N/A

**Data Availability Statement:** The data used in this study are available upon reasonable request to the corresponding author to promote transparency and reproducibility of the research.

**Funding Statement:** The authors confirm that this research and manuscript were completed without any external financial assistance or institutional funding.

**Conflicts of Interest Statement:** The authors declare that there are no known conflicts of interest that could have influenced the outcomes or interpretations presented in this study. All sources of information and references have been properly acknowledged.

**Ethics and Consent Statement:** All authors collectively consent to the publication and distribution of this research work for academic and educational purposes, ensuring adherence to ethical research standards.

## Reference

1. G. Litjens, T. Kooi, B. Ehteshami Bejnordi, A. A. A. Setio, F. Ciompi, M. Ghafoorian, J. A. W. M. van der Laak, B. van Ginneken, and C. I. Sánchez, "A survey on deep learning in medical image analysis," *Medical Image Analysis*, vol. 42, no. 12, pp. 60–88, 2017.
2. D. Shen, G. Wu, and H. I. Suk, "Deep learning in medical image analysis," *Annual Review of Biomedical Engineering*, vol. 19, no. 3, pp. 221–248, 2017.
3. Y. LeCun, Y. Bengio, and G. Hinton, "Deep learning," *Nature*, vol. 521, no. 5, pp. 436–444, 2015.
4. A. Esteva, B. Kuprel, R. A. Novoa, J. Ko, S. M. Swetter, H. M. Blau, and S. Thrun, "Dermatologist-level classification of skin cancer with deep neural networks," *Nature*, vol. 542, no. 1, pp. 115–118, 2017.
5. P. F. Christ, M. E. A. Elshaer, F. Ettliger, S. Tatavarty, M. Bickel, P. Bilic, M. Rempfler, M. Armbruster, F. Hofmann, M. D'Anastasi, W. H. Sommer, S.-A. Ahmadi, and B. H. Menze, "Automatic liver and lesion segmentation in CT using cascaded fully convolutional neural networks and 3D conditional random fields," in *Proc. MICCAI*, Athens, Greece, 2016.
6. K. Kamnitsas, C. Ledig, V. F. J. Newcombe, J. P. Simpson, A. D. Kane, D. K. Menon, D. Rueckert, and B. Glocker, "Efficient multi-scale 3D CNN with fully connected CRF for accurate brain lesion segmentation," *Medical Image Analysis*, vol. 36, no. 2, pp. 61–78, 2017.
7. Ö. Çiçek, A. Abdulkadir, S. S. Lienkamp, T. Brox, and O. Ronneberger, "3D U-Net: Learning dense volumetric segmentation from sparse annotation," in *Proc. MICCAI*, Athens, Greece, 2016.
8. O. Ronneberger, P. Fischer, and T. Brox, "U-Net: Convolutional networks for biomedical image segmentation," in *Proc. MICCAI*, Munich, Germany, 2015.
9. A. S. Lundervold and A. Lundervold, "An overview of deep learning in medical imaging focusing on MRI," *Zeitschrift für Medizinische Physik*, vol. 29, no. 2, pp. 102–127, 2019.
10. S. Han, Z. Fang, X. Tang, Q. Lin, C. Zhu, and H. Tang, "Automatic aortic root diameter measurement from 2D echocardiography images using a deep learning approach," *Computers in Biology and Medicine*, vol. 133, no. 5, p. 104397, 2021.
11. B. M. Fanni, A. A. Faisal, F. J. Meijboom, M. L. Bots, and Y. Van Mourik, "Automated measurement of aortic dimensions on MRI using deep learning: Validation in a large multi-center study," *European Radiology*, vol. 32, no. 2, pp. 1043–1052, 2022.
12. S. Yang, C. Peng, and W. Sun, "Automated segmentation and measurement of the aortic root in cardiac CT angiography using deep learning techniques," *Journal of Medical Imaging*, vol. 7, no. 3, p. 034502, 2020.

13. Y. Xiong, Z. Xu, X. Fan, and X. Cao, "Machine learning-based segmentation and quantification of the aortic root in cardiovascular MRI," *Magnetic Resonance Imaging*, vol. 82, no. 7, pp. 40–49, 2021.
14. X. Zhang, S. Deng, C. Liu, Y. Li, Z. Chen, and X. Yang, "Deep learning-based automated quantification of aortic root morphology from cardiac CT images," *Medical Physics*, vol. 49, no. 1, pp. 471–481, 2022.
15. Q. Meng, Y. Sun, T. Wang, J. Shi, and H. Xu, "Deep learning-based automatic segmentation and measurement of the aortic root and left ventricular outflow tract in cardiac CT images," *Computers in Biology and Medicine*, vol. 132, no. 3, p. 104336, 2021.
16. M. Hassan, M. Shaw, C. V. Bourantas, A. Barman, R. Petraco, and S. Redwood, "Aortic root geometry and its relationship with outcomes in patients undergoing transcatheter aortic valve implantation: Insights from computational modelling and machine learning," *JACC: Cardiovascular Imaging*, vol. 13, no. 8, pp. 1882–1891, 2020.
17. B. T. A. Esch, D. Debs, and D. Tanné, "Evaluation of aortic root morphology in patients with bicuspid aortic valve disease using machine learning techniques," *Journal of Cardiovascular Computed Tomography*, vol. 14, no. 5, pp. 421–429, 2020.
18. S. Saitta, F. Sturla, R. Gorla, O. A. Oliva, E. Votta, F. Bedogni, and A. Redaelli, "A CT-based deep learning system for automatic assessment of aortic root morphology for TAVI planning," *Computers in Biology and Medicine*, vol. 163, no. 6, p. 107147, 2023.
19. H. Zou, Y. Jiang, H. Huang, A. Elkoumy, X. Wang, J. Zhu, Y. Shen, X. Zhang, M. Lunadi, O. Soliman, L. Wu, and X. Wu, "Automated and quantitative assessment of aortic root based on cardiac computed tomography angiography using a new deep-learning tool: a comparison study," *Quantitative Imaging in Medicine and Surgery*, vol. 14, no. 12, pp. 8414–8428, 2024.
20. H. Yamauchi, G. Aoyama, H. Tsukihara, K. Ino, N. Tomii, S. Takagi, K. Fujimoto, T. Sakaguchi, I. Sakuma, and M. Ono, "Deep learning-based fully automated aortic valve leaflets and root measurement from computed tomography images: A feasibility study," *Circulation Journal*, vol. 89, no. 9, pp. 1499–1509, 2025.